Acta Crystallographica Section F
Structural Biology and Crystallization Communications
ISSN 1744-3091

A novel noncovalent complex of chorismate mutase and DAHP synthase from *Mycobacterium tuberculosis*: protein purification, crystallization and X-ray diffraction analysis

Mats Ökvist,[a] Severin Sasso,[b] Kathrin Roderer,[b] Peter Kast[b]* and Ute Krengel[a]*

[a]Department of Chemistry, University of Oslo, NO-0315 Oslo, Norway, and [b]Laboratory of Organic Chemistry, ETH Zurich, CH-8093 Zurich, Switzerland

Correspondence e-mail: kast@org.chem.ethz.ch, ute.krengel@kjemi.uio.no

Received 16 July 2009
Accepted 4 September 2009

Chorismate mutase catalyzes a key step in the shikimate-biosynthetic pathway and hence is an essential enzyme in bacteria, plants and fungi. *Mycobacterium tuberculosis* contains two chorismate mutases, a secreted and an intracellular one, the latter of which (MtCM; Rv0948c; 90 amino-acid residues; 10 kDa) is the subject of this work. Here are reported the gene expression, purification and crystallization of MtCM alone and of its complex with another shikimate-pathway enzyme, DAHP synthase (MtDS; Rv2178c; 472 amino-acid residues; 52 kDa), which has been shown to enhance the catalytic efficiency of MtCM. The MtCM–MtDS complex represents the first noncovalent enzyme complex from the common shikimate pathway to be structurally characterized. Soaking experiments with a transition-state analogue are also reported. The crystals of MtCM and the MtCM–MtDS complex diffracted to 1.6 and 2.1 Å resolution, respectively.

1. Introduction

The initial step of the shikimate-biosynthetic pathway of bacteria, fungi and plants is the synthesis of 3-deoxy-D-*arabino*-heptulosonate-7-phosphate (DAHP) from phosphoenolpyruvate and D-erythrose-4-phosphate catalyzed by the enzyme DAHP synthase (EC 2.5.1.54; Haslam, 1993). Six subsequent enzymatic steps lead to the central metabolite chorismate, at which point the metabolic flux diverges into several branches. The branch towards tyrosine and phenylalanine is initiated by chorismate mutase (EC 5.4.99.5), which catalyzes the Claisen rearrangement of chorismate to prephenate (Fig. 1). Animals lack the shikimate pathway and thus do not possess chorismate mutase, making this enzyme a target for the development of antibiotics, fungicides and herbicides.

Natural chorismate mutases have been found to occur with two fundamentally distinct folds. The relatively rare AroH class exhibits a homotrimeric α/β structure, whereas the more abundant AroQ class of chorismate mutases (MacBeath *et al.*, 1998) features all-α-helical folds (Lee *et al.*, 1995; Xue *et al.*, 1994; Sträter *et al.*, 1997; Ökvist *et al.*, 2006). AroQ enzymes have been further divided into subclasses α–δ

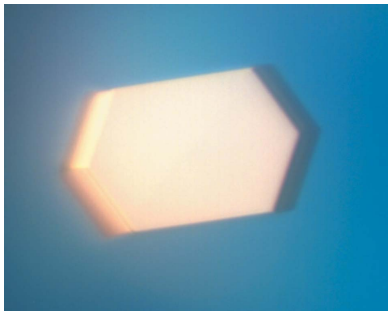

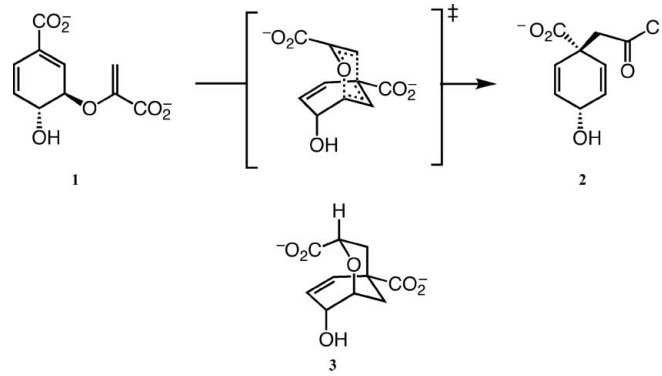

Figure 1
Chorismate mutases catalyze the conversion of chorismate (**1**) to prephenate (**2**) *via* a transition state that resembles inhibitor **3** (Bartlett & Johnson, 1985).

based on sequence comparisons (Ökvist *et al.*, 2006). *Mycobacterium tuberculosis* possesses two chorismate mutases: one is a secreted protein (*MtCM; Rv1885c) and the other is the intracellular 'housekeeping' enzyme (MtCM; Rv0948c). *MtCM and MtCM (which is the subject of this work) belong to the γ and δ subclasses of the AroQ enzymes, respectively. The $AroQ_{\delta}$ subclass exhibits several features that are very unusual for chorismate mutases, such as the absence of a number of conserved active-site residues (Sasso *et al.*, 2009). MtCM has been reported to have an unusually low catalytic activity (Kim *et al.*, 2008); however, its activity can be rescued through repositioning of active-site residues upon the addition of DAHP synthase (MtDS; Rv2178c; Sasso *et al.*, 2009).

Here, we report the production, purification and crystallization of MtCM as well as its cocrystallization with MtDS. While it is not uncommon that chorismate mutases and also DAHP synthases occur as covalent protein fusions with other enzymes, thereby acquiring regulatory potential (Ahmad & Jensen, 1986; Gu *et al.*, 1997; MacBeath *et al.*, 1998; Calhoun *et al.*, 2001; Wu & Woodard, 2006), this is the first structurally characterized noncovalent enzyme complex from the common shikimate pathway (Sasso *et al.*, 2009).

2. Experimental procedures

2.1. Preparation of intracellular chorismate mutase and DAHP synthase from *M. tuberculosis*

To structurally characterize the intracellular chorismate mutase (MtCM) and the noncovalent enzyme complex between MtCM and DAHP synthase (MtDS) from *M. tuberculosis*, sufficient amounts of pure protein had to be obtained. The 90-amino-acid MtCM (without affinity purification tag; contained in gene Rv0948c) was produced from expression plasmid pKTCMM-H (Sasso *et al.*, 2009). The 472-residue MtDS (462 amino acids encoded by Rv2178c plus the N-terminally added sequence Met-His_6-Ser-Ser-Gly serving as an affinity purification tag) was obtained by gene expression from plasmid pKTDS-HN (Sasso *et al.*, 2009). In both cases, the host for protein production was *Escherichia coli* KA13 (MacBeath & Kast, 1998; MacBeath *et al.*, 1998). KA13 is devoid of endogenous chorismate mutase activity and allows IPTG-inducible T7 RNA polymerase-directed transcription from the T7 promoter present on the gene-expression plasmids used here. Protein purity and integrity (electrophoretic homogeneity by SDS–PAGE and correct molecular mass by mass spectrometry) and concentration (using a calibrated Bradford assay; Bradford, 1976) were assessed as detailed elsewhere (Sasso *et al.*, 2009).

2.1.1. Overproduction and purification of MtCM. MtCM was overproduced by growing KA13/pKTCMM-H in LB+Amp^{150} medium in shake flasks at 303 K and 230 rev min^{-1} to the exponential phase ($0.3 \leq OD_{600} \leq 0.6$), induction with 0.5 m*M* IPTG and further incubation overnight. A cell lysate was prepared as described previously (Sasso *et al.*, 2005), but with the modification that the cells were resuspended in 50 m*M* sodium phosphate pH 6.8. The lysate was applied in portions of ~25 ml onto an FPLC Mono S HR 10/10 cation-exchange column (GE Healthcare, Otelfingen, Switzerland), which was washed with 10 ml 50 m*M* sodium phosphate pH 6.8 and then developed with 0–350 m*M* NaCl in the same buffer over 160 ml at a flow rate of 2 ml min^{-1}. Fractions containing MtCM were dialyzed against 20 m*M* piperazine pH 9.8, loaded onto a Mono Q HR 10/10 anion-exchange column (GE Healthcare) and separated with 0–250 m*M* NaCl in the same buffer over 110 ml with a flow rate of 4 ml min^{-1}. Fractions containing MtCM were concentrated and applied onto a preparative FPLC HiLoad 26/60 Superdex 75 gel-filtration column (GE Healthcare) with 20 m*M* 1,3-bis[tris(hydroxymethyl)methylamino]propane (BTP) pH 7.5, 150 m*M* NaCl as the running buffer. Fractions containing MtCM were dialyzed against 20 m*M* BTP pH 7.0. Protease-inhibitor cocktail without EDTA (catalogue No. P-8849; Sigma–Aldrich, Buchs, Switzerland) was added for storage. The final yield was 5 mg of electrophoretically homogeneous MtCM per litre of bacterial culture. Mass spectrometry confirmed the integrity of the sample (expected $[M–H]^+$, 10 091 Da; observed using MALDI-MS, 10 093 Da).

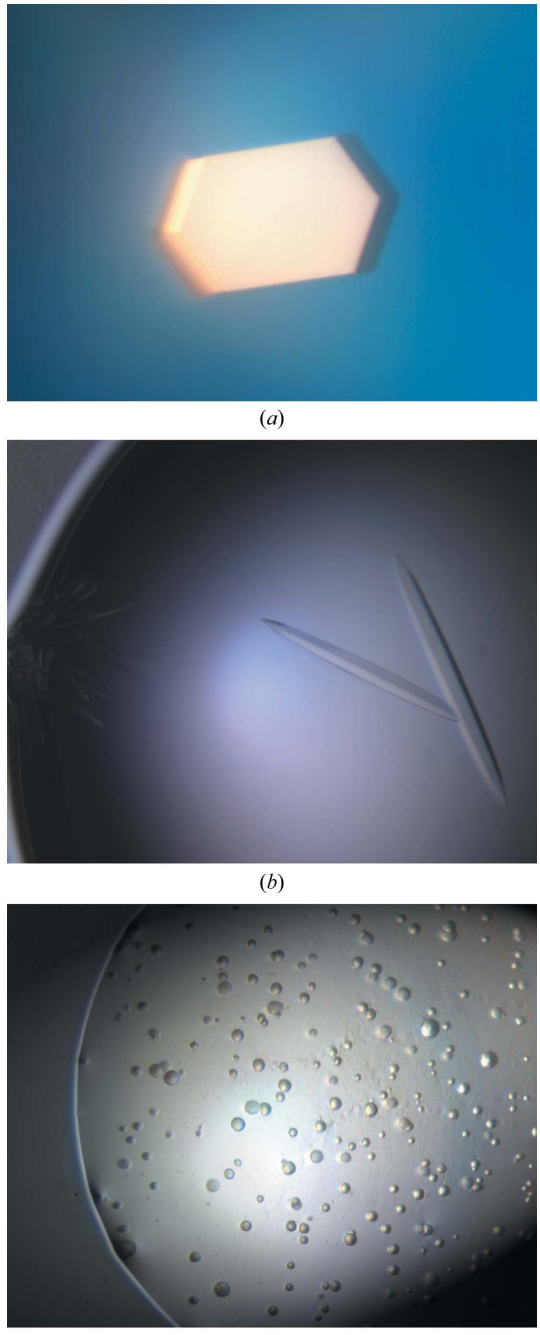

(*a*)

(*b*)

(*c*)

Figure 2
Crystals of MtCM (0.2 × 0.1 × 0.5 mm) (*a*) and the MtCM–MtDS complex (0.5 × 0.05 × 0.05 mm) (*b*) obtained under optimized conditions, the latter initially by streak-seeding from spherulites (*c*) and subsequently by streak-seeding from crystals.

2.1.2. Overproduction and purification of MtDS. MtDS was overproduced by growing a KA13/pKTDS-HN transformant in fed-batch culture in a BioFlo 3000 bioreactor (New Brunswick Scientific, Edison, New Jersey, USA) at 303 K. 2% glucose was initially added to LB+Amp[150] medium. The pH was held at 7.0 by addition of 5 *M* ammonium hydroxide and stirring was set to 500 rev min^{-1}. The cells were fed with an additional ∼5% glucose over the entire growth period. Every day, an additional 100 µg ml^{-1} sodium ampicillin and 5 m*M* ammonium sulfate were supplied. Antifoam 204 (Sigma catalogue No. A-6426) was added when necessary. After the cells had reached an OD_{600} of between 15 and 20 (after 30–56 h), the temperature was lowered to 293 K, followed by gene induction with 0.5 m*M* IPTG and further incubation overnight.

Cells were pelleted by centrifugation (10 min, 4200*g*, 277 K) and resuspended in three volumes of BTP++ consisting of 20 m*M* BTP pH 7.5, 150 m*M* NaCl, 0.5 m*M* tris(2-carboxyethyl)phosphine hydrochloride (TCEP), 0.2 m*M* phosphoenolpyruvate and 0.1 m*M* $MnCl_2$ (Webby *et al.*, 2005). After cell lysis (30 min treatment with 1 mg ml^{-1} lysozyme at 273 K, cell rupture by sonication and removal of insoluble debris by centrifugation for 20 min at 10 500*g* and 277 K), the crude extract was subjected to Ni–NTA agarose chromatography (Qiagen AG, Hombrechtikon, Switzerland) and the protein was eluted with 250 m*M* imidazole in BTP++. MtDS was further purified by a preparative FPLC HiLoad 26/60 Superdex 75 gel-filtration column with BTP++ as the running buffer. Protease-inhibitor cocktail without EDTA (catalogue No. P-8849; Sigma–Aldrich) was added for storage. An average yield of 1 mg per litre of bacterial culture was obtained of electrophoretically homogeneous MtDS with the correct mass (expected, 51 826 Da; observed using ESI-MS, 51 827 Da).

2.2. Crystallization and X-ray diffraction experiments

2.2.1. MtCM. MtCM crystals were readily obtained from a systematic grid screen (Pact Premiere, Molecular Dimensions Ltd, Newmarket, England) in a number of conditions using the hanging-drop vapour-diffusion technique at room temperature (293 K). Drops contained 0.5 µl protein solution and 0.5 µl reservoir solution and were suspended over a 50 µl reservoir. The final crystallization conditions yielding diffraction-quality crystals of MtCM (which was at a concentration of 2.45 mg ml^{-1} in BTP++ buffer) consisted of 25%(*w*/*v*) PEG 1500 and 0.1 *M* MMT buffer (Newman, 2004) pH 8–9. The crystals were tetragonal (space group $P4_32_12$), with unit-cell parameters $a = b = 62.3$, $c = 37.5$ Å. A single crystal with approximate dimensions of 0.05 × 0.05 × 0.05 mm (corresponding to part of the crystal shown in Fig. 2*a*) was used for data collection at cryogenic temperature after wet cryo-annealing using 20%(*v*/*v*) PEG 400

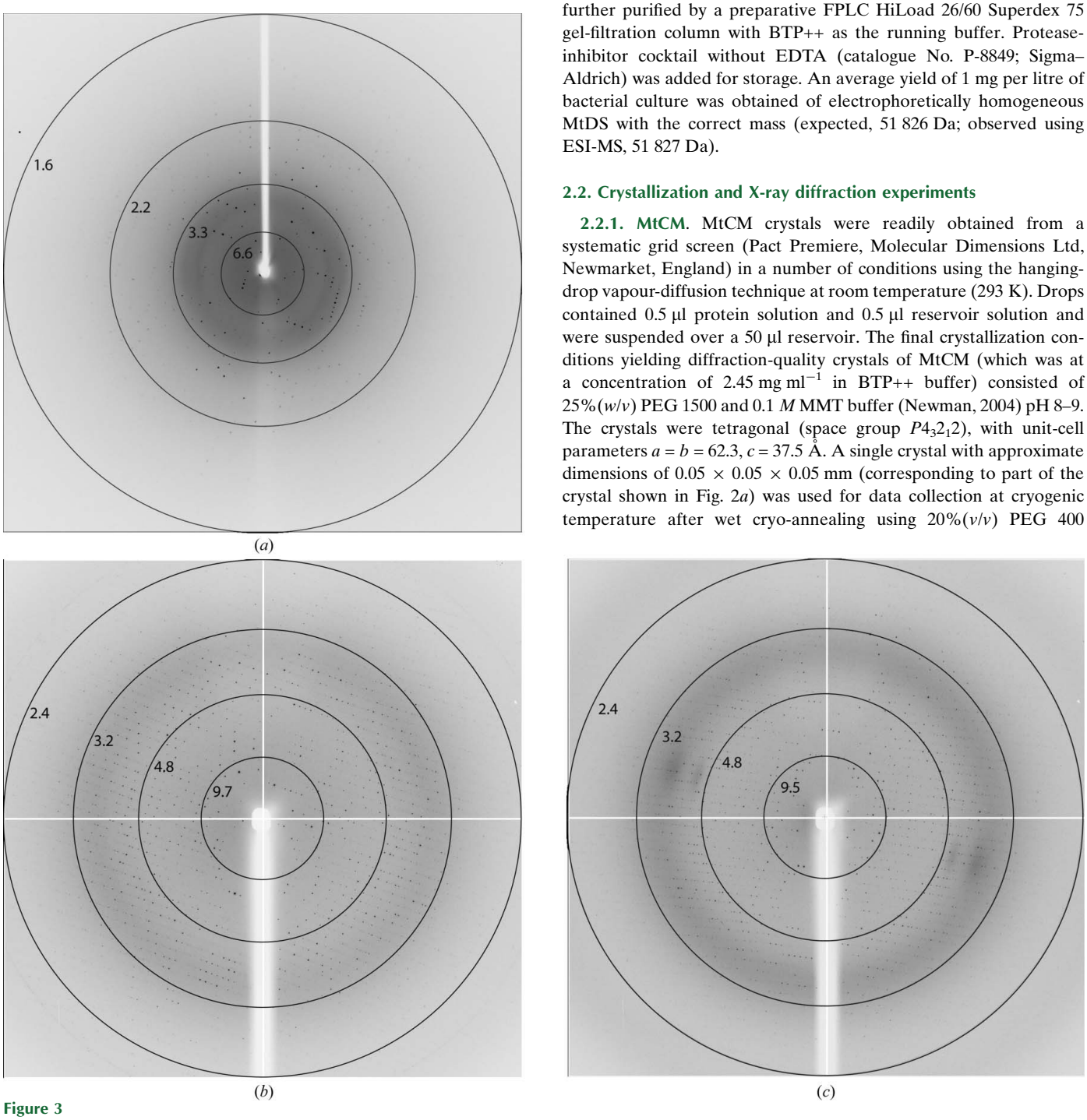

Figure 3
Diffraction images for MtCM (*a*), the MtCM–MtDS complex (*b*) and the MtCM–MtDS ternary complex with **3** (*c*) (resolution shells are indicated).

Table 1
Data-collection statistics.

Values in parentheses are for the highest resolution shell. In all cases, one crystal was used per data set.

	MtCM	MtCM–MtDS complex	MtCM–MtDS ternary complex with **3**
X-ray source	MicroMax-007HF, home laboratory source	Beamline ID14-3, ESRF	Beamline ID14-3, ESRF
Wavelength (Å)	1.54	0.931	0.931
Space group	$P4_32_12$	$P3_221$	$P3_221$
Unit-cell parameters			
$a = b$ (Å)	62.3	204.0	205.9
c (Å)	37.5	66.5	67.2
$\alpha = \beta$ (°)	90.0	90.0	90.0
γ (°)	90.0	120.0	120.0
Resolution (Å)	20.7–1.65 (1.74–1.65)	66.8–2.15 (2.27–2.15)	40.93–2.35 (2.48–2.35)
$R_{\rm merge}$†	0.046 (0.68)	0.109 (0.53)	0.105 (0.45)
$\langle I/\sigma(I)\rangle$	23.8 (2.2)	14.2 (2.5)	9.8 (2.7)
No. of reflections			
Observed	61657	569631	243808
Unique	9314	83274	67277
Multiplicity	6.6 (6.4)	6.8 (3.8)	3.6 (3.2)
Completeness (%)	99.8 (100.0)	96.6 (81.0)	98.9 (95.4)
Wilson B estimate (Å^2)	25.9	26.1	34.7
PDB code	2vkl	2w19	2w1a

† $R_{\rm merge} = \sum_{hkl}\sum_i |I_i(hkl) - \langle I(hkl)\rangle| / \sum_{hkl}\sum\langle I(hkl)\rangle$.

(added to the reservoir solution) as a cryoprotectant. Data covering 90° of reciprocal space were collected in 0.5° steps on a Rigaku MicroMax-007HF X-ray generator with an R-AXIS IV image-plate detector to a resolution of 1.65 Å (Fig. 3*a*). Data were processed with *MOSFLM* (Leslie, 1992) and *SCALA* (Evans, 2006) from the *CCP*4 program suite (Collaborative Computational Project, Number 4, 1994). Data statistics are summarized in Table 1.

In addition, MtCM crystals with slightly different unit-cell parameters have also been obtained under conditions described elsewhere (Kim *et al.*, 2008).

2.2.2. MtCM–MtDS complex. Initial crystallization conditions for the MtCM–MtDS complex were obtained from the Protein Complex Screen (Qiagen; Radaev *et al.*, 2006). Setups were performed in a 96-well sitting-drop plate, pipetting 0.5 µl of a 1:1 molar mixture of MtCM and MtDS (at a concentration of 30 µ*M* in BTP++ buffer, corresponding to final concentrations of 0.3 mg ml^{-1} MtCM and 1.5 mg ml^{-1} MtDS) onto 0.5 µl reservoir solution. After two months, the initial screening yielded one crystal from conditions consisting of 1.0 *M* ammonium sulfate and 0.1 *M* Tris–HCl pH 8.0. The rod-shaped crystal had an approximate cross section of 50 × 50 µm and a length of 300 µm. The crystal was flash-cooled in liquid nitrogen after the addition of 30% glycerol to the reservoir solution for cryoprotection and a data set was collected to 2.15 Å resolution on ESRF beamline ID14-3. The structure was solved by molecular replacement using one protomer of the previously solved MtDS structure (PDB code 2b7o; Webby *et al.*, 2005) as a search model. Initial electron-density maps revealed that the manganese centre had been damaged, either before cryoprotection and flash-cooling or in the high-energy X-ray beam, necessitating the production of additional crystals. Attempts to reproduce the original crystallization conditions only yielded spherulites (Fig. 2*c*). However, diffraction-quality crystals could be reproducibly obtained using the spherulites as seed stock and streak-seeding into hanging drops containing a 1:1 molar mixture of MtCM and MtDS (at a concentration of 30 µ*M* in BTP++ buffer, as in the initial experiments) with or without a 2:1 molar excess of transition-state analogue **3** (Fig. 1) relative to MtCM and equilibrating against a reservoir (0.5 ml) consisting of 0.9 *M* ammonium sulfate, 0.1 *M* Tris–HCl pH 7.9–8.0 and 1–5%(*v*/*v*) PEG 400 or glycerol. Using the hanging-drop technique in combination with seeding and increasing the initial drop size to 6 µl yielded rod-shaped crystals with a cross section of up to 75 × 75 µm and a length of up to 800 µm (Fig. 2*b*).

The crystals are trigonal (space group $P3_221$), with unit-cell parameters $a = b = 204.0$, $c = 66.5$ Å for the unliganded MtCM–MtDS complex and unit-cell parameters $a = b = 205.9$, $c = 67.2$ Å for the ternary complex with **3**. Diffraction data (Figs. 3*b* and 3*c*) were collected in two passes on beamline ID14-3 at the ESRF and were processed with *MOSFLM* (Leslie, 1992; Collaborative Computational Project, Number 4, 1994) and *SCALA* (Evans, 2006; Collaborative Computational Project, Number 4, 1994). Statistics for the final data sets are given in Table 1.

3. Summary and conclusion

Two *M. tuberculosis* enzymes, the intracellular chorismate mutase (MtCM) and DAHP synthase (MtDS), were overproduced in *E. coli* and purified. The purity and integrity of the samples was verified by SDS–PAGE and mass spectrometry. MtCM was crystallized alone and in complex with MtDS (the first enzyme of the shikimate pathway), which has been shown to boost the catalytic efficiency of MtCM by >100-fold (Sasso *et al.*, 2009). The crystals diffracted to 1.6 and 2.2 Å resolution, respectively, and high-quality data sets have been collected. Structure factors have been deposited in the Protein Data Bank (Berman *et al.*, 2000) under accession codes 2vkl, 2w19 and 2w1a. The crystals of the MtCM–MtDS complex are isomorphous to the crystals of free MtDS (Webby *et al.*, 2005).

This study reports the first successful crystallization of a non-covalent complex of common shikimate-pathway enzymes and has provided a foundation for exploring the molecular basis of the activation mechanism of MtCM (Sasso *et al.*, 2009). This knowledge may be useful in guiding rational drug design for severe bacterial diseases such as tuberculosis.

We thank the staff at the ESRF for beamline support and Dr R. Pulido for synthesizing inhibitor **3**. This work was funded by Novartis Pharma, the ETH Zurich, the University of Oslo and the Swiss National Science Foundation (grant No. 3100A0-116475/1).

References

Ahmad, S. & Jensen, R. A. (1986). *Trends Biochem. Sci.* **11**, 108–112.
Bartlett, P. A. & Johnson, C. R. (1985). *J. Am. Chem. Soc.* **107**, 7792–7793.
Berman, H. M., Westbrook, J., Feng, Z., Gilliland, G., Bhat, T. N., Weissig, H., Shindyalov, I. N. & Bourne, P. E. (2000). *Nucleic Acids Res.* **28**, 235–242.
Bradford, M. M. (1976). *Anal. Biochem.* **72**, 248–254.
Calhoun, D. H., Bonner, C. A., Gu, W., Xie, G. & Jensen, R. A. (2001). *Genome Biol.* **2**, 30.01–30.16.
Collaborative Computational Project, Number 4 (1994). *Acta Cryst.* D**50**, 760–763.
Evans, P. (2006). *Acta Cryst.* D**62**, 72–82.
Gu, W., Williams, D. S., Aldrich, H. C., Xie, G., Gabriel, D. W. & Jensen, R. A. (1997). *Microb. Comp. Genomics*, **2**, 141–158.
Haslam, E. (1993). *Shikimic Acid: Metabolism and Metabolites.* New York: John Wiley & Sons.
Kim, S.-K., Reddy, S. K., Nelson, B. C., Robinson, H., Reddy, P. T. & Ladner, J. E. (2008). *FEBS J.* **275**, 4824–4835.
Lee, A. Y., Karplus, P. A., Ganem, B. & Clardy, J. (1995). *J. Am. Chem. Soc.* **117**, 3627–3628.
Leslie, A. G. W. (1992). *Jnt CCP4/ESF–EACBM Newsl. Protein Crystallogr.* **26**.
MacBeath, G. & Kast, P. (1998). *Biotechniques*, **24**, 789–794.
MacBeath, G., Kast, P. & Hilvert, D. (1998). *Biochemistry*, **37**, 10062–10073.
Newman, J. (2004). *Acta Cryst.* D**60**, 610–612.

Ökvist, M., Dey, R., Sasso, S., Grahn, E., Kast, P. & Krengel, U. (2006). *J. Mol. Biol.* **357**, 1483–1499.
Radaev, S., Li, S. & Sun, P. D. (2006). *Acta Cryst.* D**62**, 605–612.
Sasso, S., Ökvist, M., Roderer, K., Gamper, M., Codoni, G., Krengel, U. & Kast, P. (2009). *EMBO J.* **28**, 2128–2142.
Sasso, S., Ramakrishnan, C., Gamper, M., Hilvert, D. & Kast, P. (2005). *FEBS J.* **272**, 375–389.
Sträter, N., Schnappauf, G., Braus, G. & Lipscomb, W. N. (1997). *Structure*, **5**, 1437–1452.
Webby, C. J., Baker, H. M., Lott, J. S., Baker, E. N. & Parker, E. J. (2005). *J. Mol. Biol.* **354**, 927–939.
Wu, J. & Woodard, R. W. (2006). *J. Biol. Chem.* **281**, 4042–4048.
Xue, Y., Lipscomb, W. N., Graf, R., Schnappauf, G. & Braus, G. (1994). *Proc. Natl Acad. Sci. USA*, **91**, 10814–10818.